

# Speckle Reduction In Ultrasound Images Of Atherosclerotic Carotid Plaque

C. Loizou<sup>1</sup>, C. Christodoulou<sup>2</sup>, C. S. Pattichis<sup>3</sup>, R. Istepanian<sup>4</sup>, M. Pantziaris<sup>2</sup>, A. Nicolaides<sup>2</sup>

<sup>1</sup> Dep. of Computer Science, Intercollege Limassol Campus, P. O. Box 51604, CY-3507 Limassol-Cyprus, e-mail: christosl@lim.Intercollege.ac.cy,

<sup>2</sup> Cyprus Institute of Neurology and Genetics, Nicosia-Cyprus, e-mail: cschr2@ucy.ac.cy, <sup>3</sup> Dep. of Computer Science, University of Cyprus, e-mail: pattichi@ucy.ac.cy, <sup>4</sup> Dept. of Electronic and Computer Engineering, Brunel University, e-mail: Robert.Istepanian@brunel.ac.uk

## ABSTRACT

The objective of this work was to develop six speckle reduction-filtering techniques and evaluate them together with texture analysis in the assessment of 240 ultrasound images of the carotid artery. The de-speckled filters are based on anisotropic diffusion, local statistics with higher moments, and geometric filtering. Results showed that some improvement in class separation (between symptomatic and asymptomatic plaques) of the images was evident after de-speckle filtering.

## 1. INTRODUCTION

Ultrasound (US) imaging being non-invasive is a powerful diagnostic tool in medicine [1]-[6]. Speckle, a form of multiplicative noise corrupts medical US imaging making visual observation difficult [2], [7]-[8]. Even radiologists with sufficient experience may not often draw useful conclusions from this texture. From an engineering point of view, speckle is most often considered a dominant source of noise in US and therefore should be filtered out [2], [7], [9]-[10]. For images that contain speckle, enhancing the image by removing the speckle without destroying important features is the goal. There are mainly three categories of speckle reduction techniques:

- 1) Techniques which operate in 3x3, 5x5 or larger pixel moving windows utilizing the statistical properties of the image neighbourhood. These can be separated into three broad categories [1]-[7]: a) Those utilizing the statistical properties, such as the first (mean) and the second moment (variance- $\sigma^2$ ) in a neighbourhood. b) Those utilizing the higher statistical properties such as the third moment ( $\sigma^3$ ) and/or the fourth moment ( $\sigma^4$ ) over a pixel neighbourhood. c) Geometric techniques, which are non-linear iterative algorithms. All the speckle filters discussed in this paper fall into this category.
- 2) Techniques utilizing the frequency spectrum of the image, which have been proved not to be very useful for speckle reduction or image enhancement and restoration [4], [7], [10]-[12].
- 3) Averaging of uncorrelated images obtained from different spatial positions, a procedure that is computational costly. Also multiple images from the same object are required [1]-[6].

The majority of the techniques presented in the literature have certain limitations: a) They are sensitive to the size and shape of the window. b) They do not enhance edges-they only inhibit smoothing near edges. c) They are not directional in the sense that in the presence of an edge, all smoothing is precluded. Instead of inhibiting smoothing in directions perpendicular to the edge are encouraging smoothing in directions

parallel to the edge. d) The thresholds used in the filtering process are insufficient in the window-based approaches [7], [13]-[14].

The objective of this study was to develop new speckle reduction techniques, investigate their performance on US images and evaluate them through a number of texture descriptors extracted from the original and filtered images. Our results show that the class separation between symptomatic and asymptomatic US images of the carotid artery are, slightly better after filtering.

In the following section, theoretical concepts of the proposed de-speckle filters are presented. In section three, filter analysis and evaluation carried out using 17 different texture descriptors are discussed. Section four and five give the results, and concluding remarks respectively.

## 2. DE-SPECKLE FILTERS

In this section, the following de-speckle filters are introduced: 2.1 *speckle* and *amnoise* using first order local statistics such as the mean and the variance, 2.2 *rtf* utilising anisotropic diffusion and the filter *anisodiff* utilising speckle anisotropic diffusion, 2.3 *momente* using local statistics with higher statistical moments such as the skewness and kurtosis of the histogram, and 2.4 the geometric filter *speck*.

### 2.1 Local statistic filters (*speckle*, *amnoise*)

Most of the introduced techniques for speckle reduction in the literature use local statistics. Their working principle may be described by a weighted average calculation using sub region statistics to estimate statistical measures over pixel windows (typically 3x3, 5x5, 7x7 sliding pixel windows). They all assume that the speckle noise model has the following multiplicative form (x denotes multiplication) [2]:

$$g_{i,j} = f_{i,j} \times n_{i,j} \quad j, i \in N \quad (2.1.1)$$

where  $g_{i,j}$  represents the noise pixel in the middle of the moving window,  $f_{i,j}$  represents the noise-free pixel and  $n_{i,j}$  is a Rayleigh distributed noise on pixel.

Hence the algorithms in this class may be traced back to the following equation [2]:

$$f_{i,j} = \bar{g}_{i,j} + k_{i,j} \times [g_{i,j} - \bar{g}_{i,j}] \quad (2.1.2)$$

where  $f_{i,j}$  is the new estimated pixel,  $g_{i,j}$  is the old pixel in the middle of a moving window,  $\bar{g}_{i,j}$  is the local mean value of a  $N_1 \times N_2$  region,  $k_{i,j}$  is a weighting factor with  $k \in [0..1]$ , and  $i, j$  the absolute pixel coordinates. The factor  $k_{i,j}$  is a function of the local statistics in a moving window. It can be found in the literature [2], [7] and is derived as:

$$k_{i,j} = [1 - \bar{g}_{i,j}^2 \times \sigma^2] / [\sigma^2 \times (1 + \sigma_n^2)] \quad (2.1.3)$$

$$k_{i,j} = \sigma^2 / [\bar{g}_{i,j}^2 \times \sigma^2 + \sigma_n^2] \quad (2.1.4)$$

for filter *amnoise* and *speckle* respectively. The values  $\sigma^2$  and  $\sigma_n^2$  represents the variance and the noise variance in the moving window respectively. If the value of  $k_{i,j}$ , with  $i, j$  the pixel co ordinates of the central pixel in a moving window, is 1 this will result to an unchanged pixel, however a value of 0 replaces the actual pixel by the local average  $\bar{g}_{i,j}$  over a small region of interest. Equation (2.1.2) is applicable both for additive and multiplicative noise by using different calculations of  $k_{i,j}$  as shown in (2.1.3)-(2.1.4).

## 2.2 Speckle Anisotropic Diffusion (*anisodiff, rtd*)

The speckle reducing anisotropic diffusion, *anisodiff* [13] uses two seemingly different methods, namely the Lee and the Frost diffusion filters [13]. A more general updated function for the output image by extending the PDE versions of the de-speckle filters is:

$$f(m, n) = g(m, n) + 1 / (N_1 \times N_2) \times \text{div}[c(C_{m,n}) \times \nabla I_{m,n}] \quad (2.2.1)$$

The function  $c(\ )$  is a bounded non negative decreasing measure. As with conventional anisotropic diffusion  $c(\ )$  is the diffusion coefficient.  $C_{m,n}$  is the coefficient of variation, in speckle filtering. For the discrete case an instantaneous coefficient of variation can be derived as follows [13]:

$$C_{m,n}^2 = (1/2) \times |\nabla I_{m,n}|^2 - (1/16) \times (\nabla^2 I_{m,n})^2 / [g(m, n) + (1/4) \times \nabla^2 I_{m,n}]^2 \quad (2.2.2)$$

It is required that  $C_{m,n} \geq 0$ . The above instantaneous coefficient of variation combines a normalized gradient magnitude operator and a normalized Laplacian operator to act like an edge detector for speckle imagery. High relative gradient magnitude and low relative Laplacian tend to indicate an edge. The filter *anisodiff* utilises speckle reducing anisotropic diffusion after 2.2.1, while the filter *rtd* utilises the traditional diffusion [13].

## 2.3 Local statistics with higher moments (*momente*)

This new technique utilizes the higher statistical moments of the image and the entropy in the local moving window. The variance in every window is a function of the 2<sup>nd</sup>, 3<sup>rd</sup> and the 4<sup>th</sup> moment and will be calculated as follows:

$$\text{variance} = 1 / (c_2 + c_3 + c_4) \times (c_2 \times \text{var} + c_3 \times m_3 + c_4 \times m_4) \quad (2.3.1)$$

with  $\text{var}$ ,  $m_3$ ,  $m_4$ , the variance, 3<sup>rd</sup> and 4<sup>th</sup> moment in a sliding pixel window. The constants  $c_2$ ,  $c_3$ ,  $c_4$  may be calculated using the measure [2]:

$$R = 1 - [1 / (1 + \sigma^2)] \quad (2.3.2)$$

which is the smoothness of the image. The higher moments will be then weighted with a factor  $c$ , which can take values  $0 < c < 1$ . The above equation will be applied in areas where:

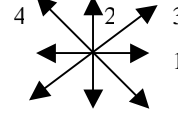
$$c_3 \times m_3 \leq c_2 \times \text{var} \leq c_4 \times m_4 \quad (2.3.3)$$

In other areas where (2.3.3) is not true, the variance parameter will be calculated as:

$$\text{variance} = 1 / (c_2 + c_4) \times (c_2 \times \text{var} + c_4 \times m_4) \quad (2.3.4)$$

## 2.4 Geometric Filter (*speck*)

This is a powerful nonlinear geometric filter that filters the multiplicative noise by utilizing the local statistics of the image [16]. It operates in four different directions, (horizontally, vertically, 2 diagonal directions):



The filter calculates the minimum and the maximum intensities for every direction in every sliding window (3x3, 5x5, 7x7 pixel window). The pixel in the middle of the window is then replaced by taking in considerations the noise component in image and adding or subtracting from the minimum and maximum intensities a noise factor. Usually the speckle index can be changed from 1 to 0.634 after the second iteration of the filter. The filter performs very well by repeated application on the image (3-4 iterations).

## 3. TEXTURE ANALYSIS FOR FILTER EVALUATION

Texture contains important information, which is used by humans for the interpretation and analysis of many types of images. It may provide useful information about the plaque characterization in US images [15]. We have used 17 different texture features [15], which were extracted from the original and the filtered images to evaluate quantitatively and qualitatively the performance of each filter: (a) **First Order Statistics (FOS)** [15]: 1) Mean value, 2) Median value, 3) Standard Deviation, 4) Skewness, and 5) Kurtosis. (b) **Spatial Gray Level Dependence Matrices (SGLDM)** The spatial gray level dependence matrices as proposed by Haralick et al. [18] were computed: 1) Angular second moment, 2) Contrast, 3) Correlation, 4) Sum of squares: variance, 5) Inverse difference moment, 6) Sum average, 7) Sum variance, 8) Sum entropy, 9) Entropy, 10) Difference variance, 11) Difference entropy, and 12), 13) Information measures of correlation. (c) **Neighbourhood Gray Tone Difference Matrix (NGTDM)** [17] 1) Coarsen, 2) Busyness, 3) Entropy, and 4) Complexity.

In order to identify the best features for the classification, the distance between symptomatic and asymptomatic plaques was calculated for the set of all images, before and after de-speckle filtering for each feature as follows:

$$\text{dis} = (|m_1 - m_2| / (\sigma_1 + \sigma_2)) \times 100 \quad (3.1)$$

where  $m_1$  and  $m_2$  are the mean values and  $\sigma_1$  and  $\sigma_2$  are the standard deviations of the two classes (symptomatic, asymptomatic). The best features are the ones with the greatest distance values [15]. If the distance after the speckle filtering is increased i.e.:

$$\text{dis}_{\text{filtered}} > \text{dis}_{\text{original}} \quad (3.2)$$

then the classes may be better separated.

In order to evaluate all the above filters we have chosen to de-speckle 240 US images (120 symptomatic and 120 asymptomatic) of carotid atherosclerotic plaques with six of our best de-speckle filters.

For each filter, a score was computed as the average distance between all the filtered and original (or noise) image features as follows:

$$\text{Score} = \frac{(\text{filtered image feature} - \text{original (or noise) image feature})}{(\text{original (or noise image feature)})} \times 100 \quad (3.3)$$

It should be noted that for mean, median, fourth moment and entropy a positive distance shows improvement, whereas for second moment, third moment and speckle index a negative distance shows improvement.

#### 4. RESULTS

The performance of the proposed filters was evaluated using equation (3.1). In the first part, de-speckle filtering was evaluated on an artificial carotid image corrupted by multiplicative noise. Figure 1(a) shows an artificial image of the carotid artery corrupted by speckle noise with a noise variance of  $\sigma_n=0.24$ . The six de-speckle filters were applied to Fig. 1(a) and the results of two of the best de-speckle filters, *amnoise* and *momente* (see also Table I) are shown in Fig. 1(b) and (c) respectively. They show an improved smoothing after filtering.

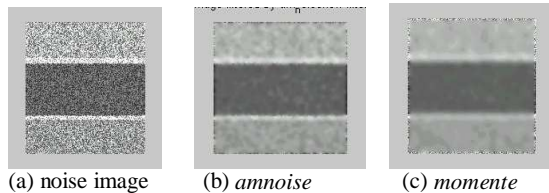


Fig. 1 De-speckle filtering on an artificial carotid image.

Table I shows the results of statistical features for Fig. 1(a) according to equation (3.1). These are the mean, median, variance ( $\sigma^2$ ), 3<sup>rd</sup> moment ( $\sigma^3$ ), 4<sup>th</sup> moment ( $\sigma^4$ ), entropy, and speckle-index (C). The number of iterations for each filter is shown at the second row of Table I. The first column gives the statistics for image in Fig. 1(a), whereas the rest of the columns give the results of equation (3.3). All filters, managed after 7, 30, 4, 10, 3, and 4 iterations respectively to reduce the variance while preserving the mean and the median. The values in bold in Table I show an improvement of the corresponding statistical feature after filtering.

All filters reduced the speckle index C, significantly thus increasing the signal to noise ratio  $\gamma=1/C$ . The skewness ( $\sigma^3$ ) becomes smaller for all of the filters, whereas the kurtosis ( $\sigma^4$ ) of the histogram becomes smaller for the filters *anisodiff*, *speck* and *speckle*, thus increasing the contrast of the image. The entropy, which is a measure of the amount of information in an image, becomes negative thus information is lost after filtering for all filters, with best filters the *speckle* and *momente*. The last row of Table I shows the Score of all features as introduced in (3.3). The best filter is the one with the

highest score, which is the *amnoise* followed by *anisodif*.

Table I: Statistical results of an artificial carotid image. For each filter the percentage difference between the noise image and the de-speckled image is given (see equation (3.1)).

Fea ture	noise image	<i>amnoise</i>	<i>anisodif</i>	<i>momente</i>	<i>rtd</i>	<i>speck</i>	<i>speckle</i>
Nr. of It.		7	30	4	10	3	4
mean	126	<b>11</b>	<b>8</b>	<b>8</b>	<b>13</b>	<b>38</b>	<b>13</b>
median	123	<b>23</b>	<b>20</b>	<b>25</b>	<b>23</b>	<b>38</b>	<b>17</b>
$\sigma^2$	59	<b>-44</b>	<b>-37</b>	<b>-27</b>	<b>-39</b>	<b>-28</b>	<b>-33</b>
$\sigma^3$	0.25	<b>-240</b>	<b>-260</b>	<b>-188</b>	<b>-108</b>	<b>-116</b>	<b>-200</b>
$\sigma^4$	2.12	-14	<b>7</b>	-1	-21	<b>27</b>	<b>2</b>
Entropy	9.95	-34	-29	-13	-19	-17	-5
C= $\sigma/m$	0.06	<b>-33</b>	<b>-33</b>	<b>-33</b>	<b>-33</b>	<b>-50</b>	<b>-33</b>
Score		57	56	42	37	45	43

Table II is structured similarly to Table I. It shows the comparison of the results for the 240 real US images of carotid plaques. The values shown in the table represent the percentage distance between symptomatic and asymptomatic classes according to equation (3.1). The bolded values represent the values that showed an improvement after filtering. Some of our de-speckle filters, shown in Table II, are changing a number of texture features, thus increasing the distance between the classes and therefore making the identification of symptomatic and asymptomatic plaques more feasible.

Table II: Statistical analysis and texture features of 240 ultrasound images of carotid plaque. For each filter the percentage difference between the noise image and the de-speckled image is given (see equation (3.1)).

Featu re	origin al	<i>amno ise</i>	<i>aniso dif</i>	<i>mome nte</i>	<i>rtd</i>	<i>Speck</i>	<i>speck le</i>
Nr. of It.		7	30	4	10	3	4
<b>FOS</b>							
Mean	0,35	-77	-37	<b>11</b>	-23	-6	-37
Median	0,36	-64	-17	<b>6</b>	-8	-8	-17
$\sigma^2$	0,21	<b>67</b>	<b>48</b>	<b>48</b>	-14	-14	<b>48</b>
$\sigma^3$	0,26	-69	-54	-23	-31	-4	-54
$\sigma^4$	0,2	-20	-80	-40	-40	-5	-80
C	1,3	-0,11	-0,19	0,6	-0,17	-0,66	-0,19
Score		50	39	21	19	6	39
<b>SGLDM</b>							
ASM	0,33	-30	-12	<b>6</b>	-15	-12	-15
Contrast	0,26	<b>15</b>	<b>8</b>	-73	<b>8</b>	<b>12</b>	<b>15</b>
Correllat	0,29	-90	-24	-7	-10	-3	-10
SOV	0,23	<b>61</b>	<b>4</b>	<b>35</b>	-43	-13	<b>4</b>
IDM	0,38	-42	-13	<b>5</b>	-16	-5	-13
SA	0,35	-74	-29	<b>14</b>	-17	-3	-29
$\Sigma$ Var	0,24	<b>54</b>	0	<b>33</b>	-54	-13	-4
$\Sigma$ Entrop	0,39	-23	-8	<b>3</b>	-10	-5	-8
Score		65	16	29	29	11	16
<b>NGTDM</b>							
Entropy	0,39	-23	-8	<b>5</b>	-10	-3	-5
Coarsen	0,47	-34	-4	-30	-36	-2	<b>2</b>
Busynes	0,18	<b>11</b>	<b>83</b>	-44	<b>67</b>	0	<b>67</b>
Comple.	0,14	<b>129</b>	<b>50</b>	<b>43</b>	<b>50</b>	-21	<b>93</b>
Score		33	24	20	27	4	28

ASM=angular 2<sup>nd</sup> moment, SOV=Sum of squares: variance, IDM=Inverse difference moment, SA=Sum average,  $\Sigma$  Var=Sum Variance. **Bolded Values: Improvement after filtering**

The filter *momente*, shows the best results and performs even better than the filter *anisodif* by increasing the distance between classes. The filter *amnoise* shows better results than the *anisodif*. The rest of the filters show poorer performance. The results in Table II show that an improvement is evident in some of the features of the real images with best filters the *momente*, *amnoise*, *anisodif*, *speckle*, *speck* and *rtd*. Texture features, which were improved in most of the filters, are the contrast, busyness, complexity, sum of squares, variance and standard deviation. The score at the last row of every feature category shows that the best filter is *amnoise* followed by *momente*, *anisodiff*, *speckle*, *rtd* and *speck*. Fig. 2 shows some results of the proposed filters compared with *anisodiff* and *rtd*.

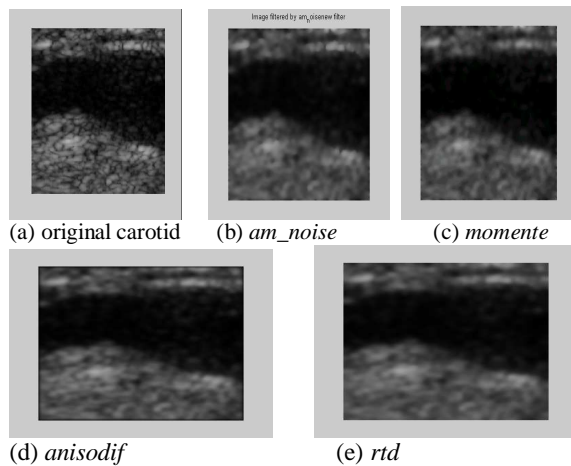


Fig. 2: De-speckled US images of carotid plaque.

## 5. CONCLUDING REMARKS

In this work we have developed six different techniques for speckle reduction and tested them on 240 ultrasound images of carotid plaque. We have evaluated the results with 17 different texture descriptors shown in Table II. Other researchers [2], [7], [10], [13], [14] have evaluated their techniques on a very limited number of US images (3-4) and tested their techniques based on a handful of texture features like the variance, the mean and the speckle index between the original and the filtered image. Y. Yongjian [13] proposed speckle reducing anisotropic diffusion as the most appropriate for images degraded by speckle but we have proved that the filters proposed in this study, *amnoise* and *momente* performed better than the proposed one as seen from the bolded values in Table II.

De-speckle filtering is an important operation in the enhancement of ultrasonic imaging of the carotid artery. Furthermore, de-speckle filtering can be used as a pre-processing step in a system for the automated segmentation of US carotid plaque images. Initial findings show some promise of these techniques, however, more work is needed to evaluate further the performance of the suggested de-speckle filters.

## References

[1] M. Sonka, J. Fitzpatrick. Handbook of Medical Imaging, Vol. 2, Med. Img. Proc. analysis, SPIE, 2000.

[2] C. Loizou. Speckle Reduktion in Medizinischer Ultraschallbildern. University of Kaiserslautern, Germany, Thesis, 1990.

[3] Al. Bovik. Handbook of Image & Video Processing. Academic Press, 2000.

[4] I. Backman. Handbook of Medical Imaging, Processing and analysis. Academic Press, 2000.

[5] K. Castleman. Digital Image Processing. Prentice Hall Inc., 1996.

[6] R Woods, R. Gonzalez. Digital Image Processing, Addison-Wesley Publishing Co., 1992.

[7] T. Greiner, C. Loizou, M. Pandit, J. Mauruschat, F.W. Albert. Speckle Reduction in Ultrasonic Imaging for medical Applications. Proc of the ICASSP91, Toronto Canada, May 14-17, 1991, pp. 2993-2996.

[8] D. Guo. Intravascular Ultrasound Speckle Statistics. Proc. of the annual meeting of the Eng. in Med. and Biology Soc., 20(2), pp. 796-799, 1998.

[9] R. Fjortof et al. A region-based approach to the estimation of local statistics in adaptive speckle filters. CESBIOToulouse Cedex, France, 2000.

[10] A. Nelson et al. Speckle noise filtering in SAR images by MAP approach. Cybernetic Vision Group IFSC-Uni. of Sao Paulo, C. Post. 369, SP, Brasil, 1991.

[11] V. Metzler et al. Restoration of Ultrasound Images by Non-linear scale-space filtering. Proc., SPIE 3961, pp. 69-80, 2000.

[12] A. Pizurica et al. De-speckling SAR images using wavelets and a new class of adaptive shrinkage estimators. IEEE 2001, ICIP Thes.-Greece, pp. 233-236

[13] Y. Yongjian, Scott T. Acton. Speckle Reducing Anisotropic Diffusion, IEEE Transactions on Image Processing, 2001, Submitted for publication.

[14] L. Gagnon. Wavelet Filtering of speckle noise – Some numerical results. Vision Interface, March 7, 1999, Trois-Rivieres, Canada, 19-21 May, pp. 336-343.

[15] C. Christodoulou et al. Multifeature -Texture Analysis for the classification of carotid plaques, in CD-ROM, Proc. Int. Joint Conference on Neural Networks IJCNN '99, Washington DC, 10-16 July 1999.

[16] L. Busse, T. R. Crimmins, J. R. Fienup. A model based approach to improve the performance of the Geometric filtering speckle reduction algorithm. IEEE Ultrasonics Symposium 1995, pp. 1353-1356.

[17] Weszka J.S., Dyer C.R., Rosenfield A., "A Comparative Study of Texture Measures for Terrain Classification", *IEEE Transactions on Systems, Man, & Cybernetics*, Vol. SMC-6, April 1976.

[18] Haralick R.M., Shanmugam K., Dinstein I., "Texture Features for Image Classification", *IEEE Transactions on Systems, Man, and Cybernetics*, Vol. SMC-3, pp. 610-621, Nov. 1973.